EXPERIMENTS AND ANALYSES OF EXPLOSION AT AN URBAN INTERSECTION

M. Johansson[1], O.P. Larsen[2], L. Laine[2]

[1]*REINERTSEN Sverige AB, Lilla Bommen 5, SE-411 13 Göteborg, Sweden*
[2]*ANKER – ZEMER Engineering A/S, P.O. Box 253, NO-0702 OSLO, Norway*

ABSTRACT

Predicting the load caused by a propagating blast wave in urban environment is a complex task. For many load cases engineering tools based on empirical data or semi-empirical methods, is sufficient. However, when the geometry gets more complex, it might be necessary to use so-called hydro code programs to calculate the effect of the blast wave. Hence, there is also a need to verify such programs against experimental results. Once validated, though, such programs may be used to better understand the effects of blast load in complex load situations.

In order to validate the results from the hydro code AUTODYN^{TM}, an experimental test series, scale 1:5, simulating an explosion in urban environment, was carried out. A simplified intersection built up of four concrete boxes, dimension 2.3 m, with a total of eight charges, 0.4 and 1.6 kg of PETN, detonated at various locations were registered using 25 pressure gauges. Numerical simulations were carried out in AUTODYN prior to the experimental test series. In order to handle the simulations, and thus decrease the calculation time needed, an automatic remapping procedure, in which the progress of the shock front was automatically taken into consideration, was developed. To compare experimental and numerical results In addition, a coherence measure was introduced. Out of almost 200 compared pressure-time relations about 65 % reached $Coh \geq 0.5$; i.e. a limit that indicates very good agreement. Consequently, it is concluded that AUTODYN manage very well to predict the blast load obtained in a complex urban environment and that it may provide a powerful tool for further blast load studies.

An approach for a simplified technique, using superposition of several incident shock waves, to estimate the blast load in a more complex environment is presented and compared to the experimental and numerical results. This simplified technique is a rather crude instrument when compared to Autodyn. However, it still provides a general idea of which blast waves sums up the resulting pressure time history, and hence may be used in an early stage to approximately describe the resulting loads on a structure. The results presented herein yield a discrepancy of the positive and negative impulse intensities of only about 20 % compared to that in the experiments.

INTRODUCTION

The Swedish Rescue Services Agency (Räddningsverket) is responsible for the building regulations of the Swedish civil defense shelters. The shelters have specific regulations for how they are planned, built, equipped and maintained [1]. It is also the responsibility of The Swedish Rescue Services Agency to maintain and develop the knowledge connected to these

structures. Consequently, a research project, [2], was initiated in 2006 wherein the main aim is to increase the knowledge of the load characteristics from a blast load and how to determine the capacity of any given building or group of buildings to withstand such loads.

Predicting the load caused by a propagating blast wave in urban environment is a complex task. According to [3] there are three types of methods to be used: empirical, semi-empirical and numerical methods. For non-complex load cases it is usually sufficient to use engineering tools based on empirical data, e.g. ConWep [4]. For more complex situations, though, it is necessary to use semi-empirical methods, i.e. methods based on models in which the important physical process is accounted for in a simplified way. Several researchers have also developed such models, e.g. [5]-[9], that work well within given limits and that provides an increased understanding of the resulting blast load. However, when the geometry gets more complex, such as in an urban environment, it may no longer be enough to use this type of simplified tools, [10]. In such cases numerical methods incorporating computational fluid dynamics (CFD) techniques, so-called hydro codes, may be used. However, even though the computational possibilities, regarding both the complexity of the analysis and the required computer time, steadily increase, it is still of utmost importance to make sure that the results obtained in such methods correlate to the real experimental behavior. Hence, there is a need to verify such programs against experimental results. Once this is guaranteed it is possible to use hydro code programs instead of, or in conjunction with, experimental performances.

In this project the explicit code AUTODYN^{TM} [11] is used. It has previously been shown in [12] that AUTODYN provides satisfactory agreement with ConWep in analyses of spherical air bursts. However, it is also necessary to verify that this is the case in a more complex urban environment. Accordingly, when the opportunity to take part in an experimental test-series, originally initiated and planned by the Norwegian Defense Estates Agency (Forsvarsbygg) and to be carried out in cooperation with the Swedish Defense Research Agency (FOI), revealed itself the Swedish Rescue Services Agency joined in as a co-financier. The aim of this was twofold: to increase the knowledge about blast load in a complex environment and to investigate the possibility for AUTODYN to predict the resulting load characteristics obtained in such a case. Furthermore, the results obtained have also been used to compare the possibility to use a simplified semi-empirical calculation method, based on super positioning of several incident blast waves modified with regard to diffraction.

EXPERIMENTAL STUDY

The experimental location consisted of four concrete cubic boxes (dimension 2.3 m) positioned at a distance of 2.3 m apart, see Figure 1. Two types of charges, 0.4 kg PETN and 1.6 kg PETN were used and positioned either close to the ground (0.20 m) or at mid height (1.15 m) of the concrete boxes in four different locations. The tests were carried out in scale 1:5 meaning that the concrete boxes approximately corresponded to a four-story building of height 11.5 m and the small charge of 50 kg PETN, detonating 1.0 m above ground. Hence, a threat situation roughly equal to what might be expected from a small car bomb.

A total of 25 pressure gauges were used to register the pressure-time relations at various locations. 20 gauges had fixed positions in the concrete boxes: 10 low (L) at a level of 0.20 m, 8 in the center (C) at 1.15 m above the ground and 2 on the roof (R), see Figure 1. All gauges but two were positioned in the middle of the wall/roof. The last two gauges (BA6L and BA7L) were positioned low 0.20 m from one of the box corners. The remaining 5 gauges were used as free field pressure gauges (FF) and fastened on wooden boards placed on the ground, with various positions depending on the position of the charge, see Figure 2.

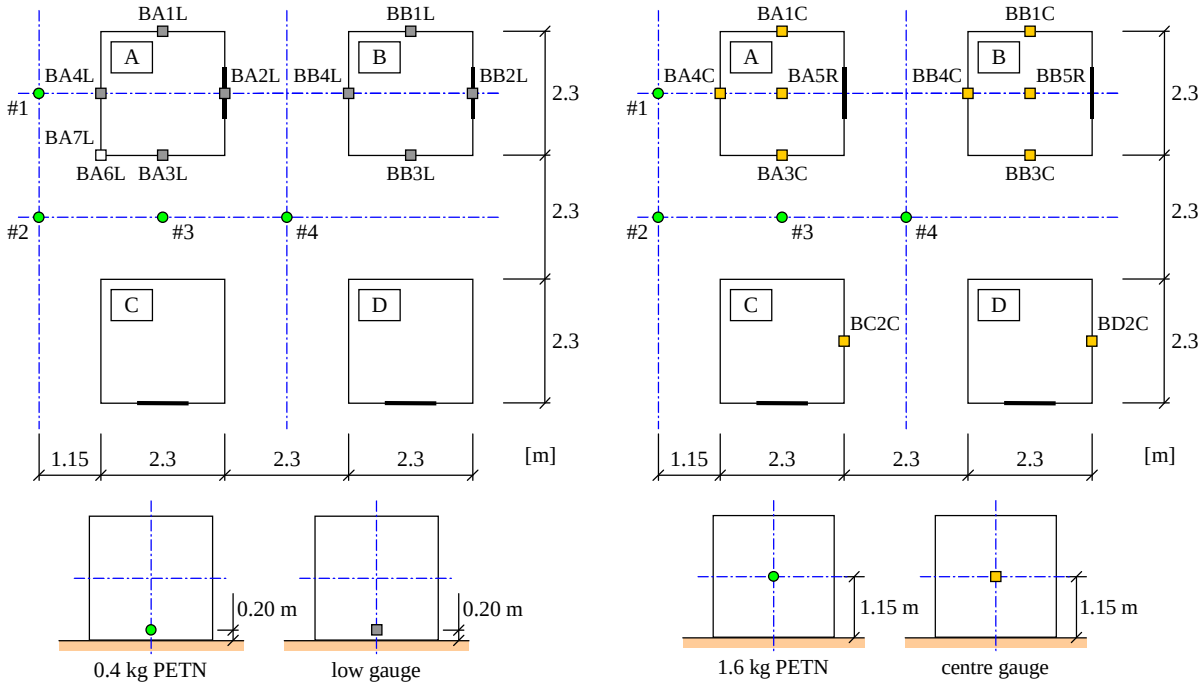

Figure 1: Top view of the experimental set-up and gauges located on the concrete boxes. The charges were placed in four different positions (#1 – #4) at a height of 0.2 m (0.4 kg PETN) or 1.15 m (1.6 kg PETN) above the ground.

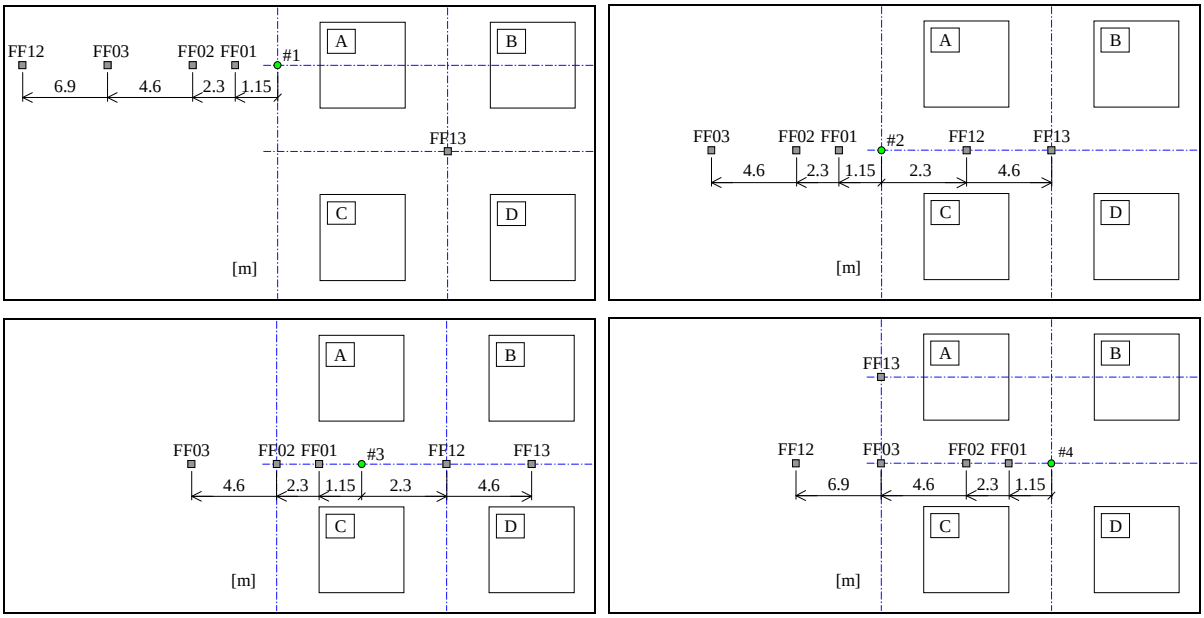

Figure 2: Top view of the different ground gauge positioning for each charge location.

The explosive used was the Swedish PETN, Sprängdeg m/46, with a density of about 1 500 kg/m^3, which consists of approximately 86 % pentolite and 14 % mineral oil. Accordingly, the 0.4 kg and 1.6 kg charges used consisted of 0.344 kg and 1.376 kg pentolite, respectively. Using the average equivalent TNT weight 1.21, given in ConWep, the scaled distance Z (expressed as TNT equivalent) can be determined. The minimum horizontal projection of the distance between the charges and the pressure gauges varied from 1.15 m to about 10 m, which provide a scaled distance of $1.5 \leq Z \leq 13$ m/kg$^{1/3}$ and $1.0 \leq Z \leq 8.5$ m/kg$^{1/3}$ for the 0.4 kg and 1.6 kg charges, respectively.

FINITE ELEMENT MODEL

The blast simulations were performed using the explicit code AUTODYN [11]. All simulations were made before the experiments were carried out, which means that the experimental results are used to validate how well AUTODYN manage to describe the blast load in a complex environment similar to that in a city.

In the numerical model the physical domain was represented by rectangular boxes in 3D which in turn were filled with cube shaped hexahedral linear elements. The size of these rectangular boxes varied based on the blast scenarios as well as the different remap stages and the planar symmetry present. A typical series of 3D remap runs over 4 stages would have approximate rectangular domain sizes of: $(2\ \text{m})^3$, $(4\ \text{m})^3$, $(8\ \text{m})^3$ and $(16\ \text{m})^3$. The element size used highly depended on the remap stage and the total number of elements employed in the numerical mesh. The high-resolution runs strove to utilize the maximum number of elements possible, i.e. approximately 4.5 million elements, which in turn yielded an element size of approximately 10 mm at the first 3D remap stage. The remapping ratio was always 1:2, consequently doubling the element size in each direction at every new remap stage. The four concrete boxes and the ground were modeled using rigid boundaries. In all but the last remapping stage no boundary conditions were necessary since the blast wave front was always fully contained inside the corresponding numerical domain. In the last stage, though, an outflow boundary condition was applied to the external boundaries of the domain.

Each simulation involved separate runs over several stages in which a self-developed automatic remapping technique was used. The first stage involved a 1D spherical symmetric run using a Multi-Material Euler solver simulating the initial detonation phase with both explosive material and air. A remap procedure was then performed into a 2D axial symmetric domain using the same Multi-Material Euler solver. Finally the simulation was concluded by a series of 3D remapping runs using an Euler-FCT solver with air only. Some of these 3D remapping stages involved planar symmetry, in which case the symmetry was fully exploited in the simulations. Figure 3 exemplify the simulation procedure for two 3D remapping stages.

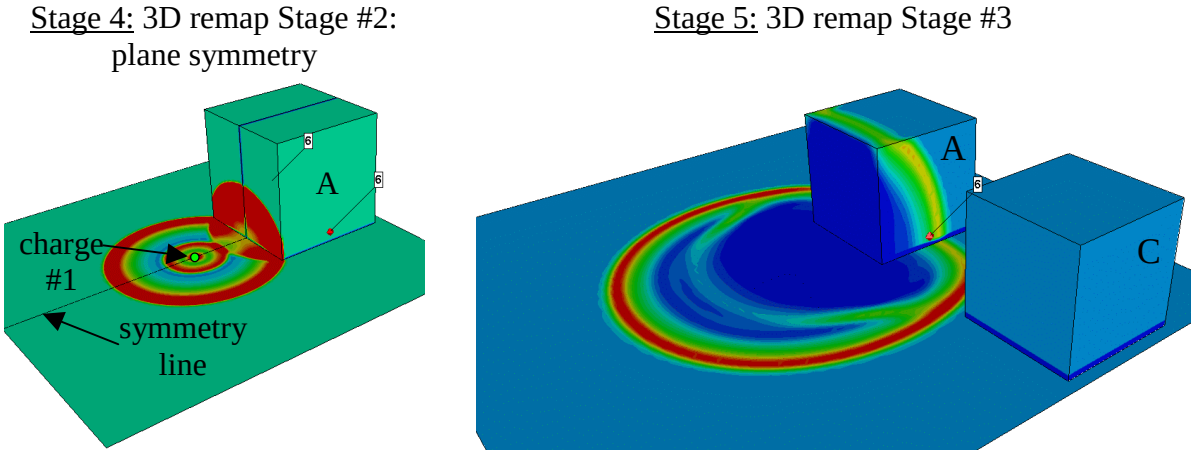

Figure 3: Illustration of the principal layout of the finite element model for simulation of charge at location #1 for Stages 4 and 5.

The large number of simulations with their accompanying remapping stages called for automation at several levels of the simulation process. Therefore, an automatic script generation with AUTODYN-linked Fortran user-subroutines was developed. The main idea of this methodology was to enable automatic detection of the shock front during the blast, so that a remap process could be initiated at the time when the shock front was close to the model rigid boundaries, i.e. concrete boxes, or the boundary of the numerical domain.

In AUTODYN there are four different pre-defined material models for the explosive PETN, where the material densities vary between 0.88 kg/m^3 and 1.77 kg/m^3. A pre-study was carried out to determine the difference between these material models and it was found that three out of four models generated almost identical results, [13], [14]. This, together with an approximation that the explosive in the charges used had a density of about 1.7 kg/m^3, [13], lead to the use of the PETN material model with density 1.77 kg/m^3 in the final AUTODYN simulations of the experimental set-up. The explosive was modeled using the JWL Equation of State (EOS) with automatic conversion into Ideal Gas EOS when the entire explosive had reached a compression value of -0.95. Additionally, at the start of the first 3D remap stage the explosive was converted into air, thus facilitating the use of the single material Ideal-Gas-EOS-Only Euler FCT solver. Input parameters for air and explosive used are listed in Table 1.

Table 1: Summary of input parameters in AUTODYN for air and explosive PETN.

Air	
ρ_0	$1.226 \cdot 10^{-3}$ (g/cm^3)
γ	1.4
P_0	101.3 (kPa)

PETN 1.77	
ρ_0	1.77 (g/cm^3)
C-J Detonation velocity	8 300 (m/s)
C-J Energy density	$1.01 \cdot 10^7$ (kJ/m^3)
C-J Pressure	$3.35 \cdot 10^7$ (kPa)

In this paper mainly the results for the 0.4 kg charges are presented. Hence, if not mentioned otherwise all results presented are related to the small charges. For more information about the experiments and the analyses carried out, see [13], [14].

RESULTS

Comparison with ConWep

A comparison of measured peak pressure in the free field gauges (FF01 to FF13) and that predicted using ConWep has been made in [13] and [14] and it was found that the correspondence was satisfactorily. As a further illustration two samples of the pressure-time relations for charges at location #1 and #4 are compared to that predicted by ConWep in Figure 4. The pressures obtained from the charge at location #1 should agree well with that of ConWep whereas it from the charge at location #4 is expected to deviate somewhat from ConWep due to confinement effects at ranges larger than about 2.3 m.

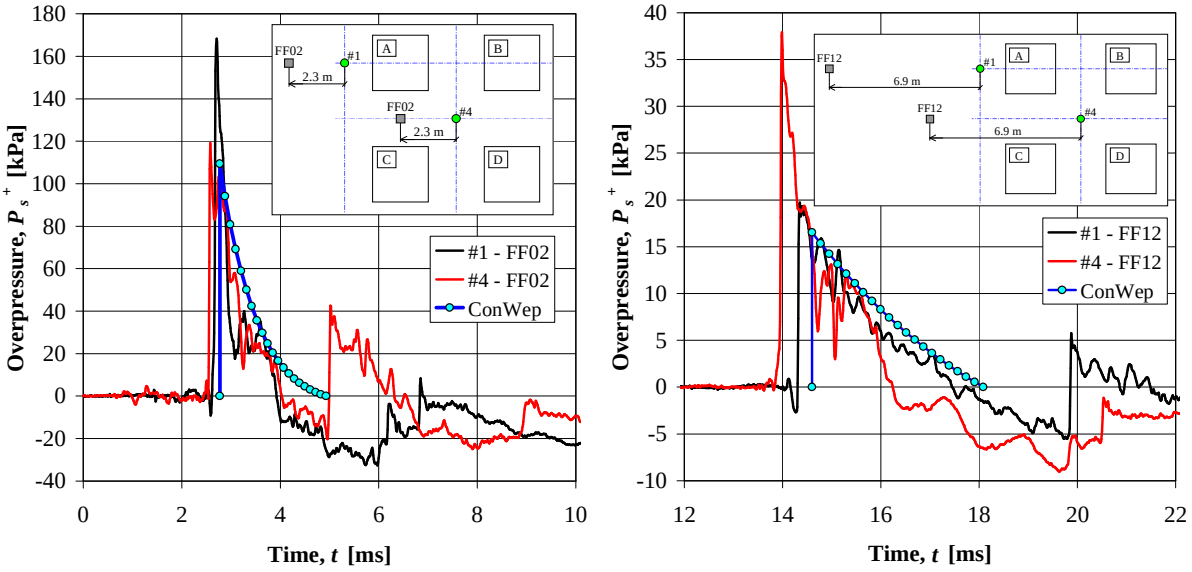

Figure 4: Comparison of pressure-time relations in the experiments and ConWep [4].

The key parameters of this comparison are summarized in Table 2. From this it can be observed that ConWep somewhat underestimate the peak pressure and overestimate the arrival time for the compared pressure relations. The resulting impulse intensity of the initial positive phase, though, is rather similar.

Table 2: Summary of blast key parameters related to pressure-time relations in Figure 4.

Gauge	R [m]	t_a [ms]	P_s^+ [kPa]	i_s^+ [Pas]	T^+ [ms]
#1-FF02	2.3	2.58	168	57	1.31
#1-FF12	6.9	14.3	20	24	3.15
#4-FF02	2.3	2.43	119	67	1.49
#4-FF12	6.9	13.8	38	29	2.41
ConWep	2.3	2.77	109	67	2.16
ConWep	6.9	14.6	17	25	3.49

It shall be observed that the peak pressure from a detonation in location #1 is noticeable higher than from that in location #4 at a distance of $R = 2.3$ m. However, at a distance of 6.9 m the opposite is true, the pressure from the blast wave originating from location #4 being higher. This effect is believed to be a result of the confinement effect obtained when the blast wave propagates in the space between the concrete boxes.

Comparison with AUTODYN

Table 3 presents a comparison of key parameters overpressure P^+, arrival time t_a and impulse intensity i^+ and i^- obtained in the AUTODYN simulations and that of the experiments for charge locations #1 and #3. Here, the impulse intensities i^+ and i^- are defined as the sum of all positive and negative phases, respectively, within the time period t_{end}.

$$i^+ = \sum_{k=1}^{n} i_k^+ = \sum_{k=1}^{n} \int_{t_{a,k}}^{t_{end,k}} P^+(t)dt \tag{1}$$

$$i^- = \sum_{k=1}^{n} i_k^- = \sum_{k=1}^{n} \int_{t_{a,k}}^{t_{end,k}} P^-(t)dt \tag{2}$$

To get a better overview of how well the results coincide a coherence measure, according to Eq. (3), was introduced.

$$Coh = 1 - \frac{\int_0^{t_{end}} \left| P_{AD}(t) - P_{Exp}(t) \right| dt}{i_{Exp}^+ + i_{Exp}^-} \tag{3}$$

Here $P_{AD}(t)$ and $P_{Exp}(t)$ are the pressure obtained in the AUTODYN simulations and experiments, respectively, while i^+_{Exp} and i^-_{Exp} are the total positive and negative impulse intensities from the experiments according to Eqs. (1) and (2) up to time $t_{end} = 50$ ms. Thereby, it is possible to fairly straightforwardly compare a large number of numerical and experimental results and get a measure of how well they coincide. Using this measure, $Coh = 1.0$ signify a perfect match. However, as illustrated in Figure 5, $Coh \geq 0.5$ corresponds to very good agreement between simulated and experimental results.

Table 3: Summary of key parameters P^+, t_a, i^+ and i^- from AUTODYN analyses and experiments for charge locations #1 and #3 when t_{end} = 50 ms. A marking "-" in the table indicate that the experimental result was not valid.

	Location #1								Location #3							
Gauge	AUTODYN				Experiments				AUTODYN				Experiments			
	P^+ [kPa]	t_a [ms]	i^+ [Pas]	i^- [Pas]	P^+ [kPa]	t_a [ms]	i^+ [Pas]	i^- [Pas]	P^+ [kPa]	t_a [ms]	i^+ [Pas]	i^- [Pas]	P^+ [kPa]	t_a [ms]	i^+ [Pas]	i^- [Pas]
FF01	656	0.62	143	137	480	0.65	248	-	698	0.62	226	184	610	0.61	237	704
FF02	129	2.42	85	94	168	2.58	57	-	136	2.38	140	141	93	2.53	120	220
FF03	32	7.69	52	50	47	8.14	82	54	33	7.74	76	77	45	7.78	71	66
FF12	14	13.45	35	35	20	14.27	38	35	136	2.38	137	141	93	2.63	113	155
FF13	16	9.89	32	32	18	10.50	28	31	34	7.61	114	112	37	8.21	106	102
BA1L	51	3.71	61	67	-	-	-	-	8	9.71	52	51	8	9.81	49	47
BA2L	7	9.63	49	48	8	10.28	53	49	52	3.73	113	115	40	3.90	110	116
BA3L	51	3.71	113	115	63	3.89	112	110	2 258	0.63	505	235	2 369	0.47	763	328
BA4L	2 100	0.63	461	208	1 745	0.63	429	-	52	3.73	70	73	58	3.81	73	74
BA6L	94	1.56	76	148	114	1.68	104	107	1 272	1.05	325	233	991	1.03	345	238
BA7L	1 221	1.05	290	211	599	1.02	187	452	103	1.61	70	132	146	1.65	72	174
BB1L	6	15.34	20	22	11	16.76	22	19	8	11.55	34	31	8	12.34	32	27
BB2L	3	22.00	21	20	3	23.35	23	20	5	13.52	33	35	5	13.85	32	33
BB3L	6	15.34	42	44	11	16.63	45	44	51	7.93	115	112	54	8.39	99	98
BB4L	14	13.41	68	70	-	-	-	-	77	6.45	131	127	73	6.89	122	118

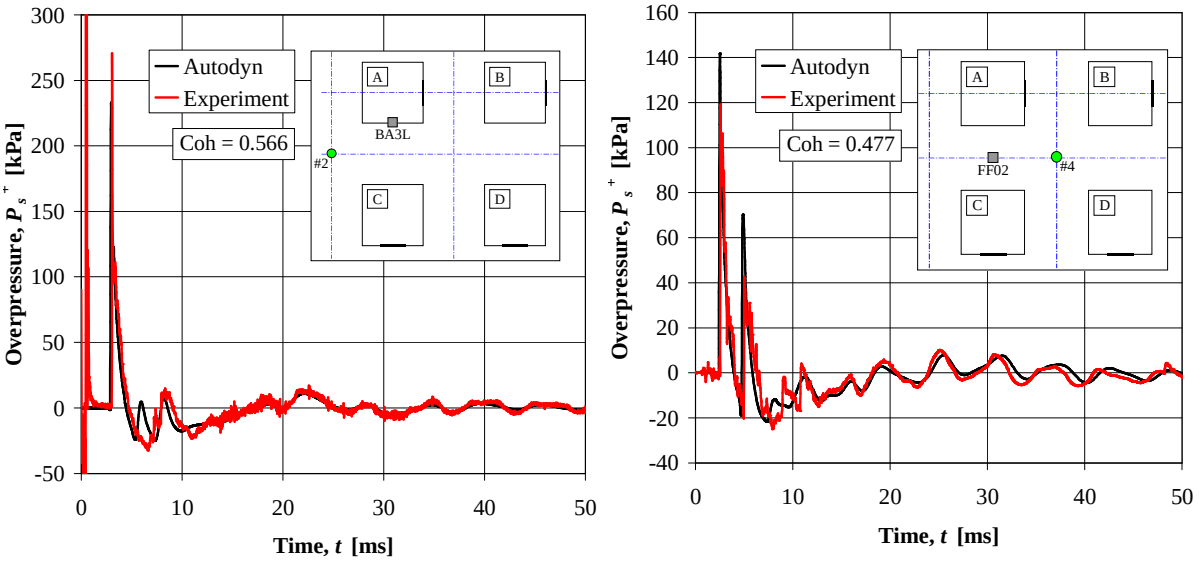

Figure 5: Example of correlation between AUTODYN analyses and experiments: #2-BA3L (left) with *Coh* = 0.566, and #4-FF02, with *Coh* = 0.477.

From Table 3, Figure 5 and further comparisons presented later in this paper it can be seen that the agreement between experimental and numerical results is generally very good. The similarities between the pressures measured in the experiments and those obtained in AUTODYN is evident. It can be concluded, though, that the rapid pressure rise observed in the experiments is not always fully captured in AUTODYN. This is due to the model discretization; i.e. the use of several remapping stages cause loss of information and also leads to an element mesh that is no longer fine enough to accurately capture rapid pressure changes. Nevertheless, the general behavior is still captured with good accuracy. Furthermore, it was observed that the agreement between analyses and experimental results increased when the pressure decreased. Thus, when the pressure was reduced to less than about 50-100 kPa the general agreement went from very good to excellent. In Figure 6 the complete batch of

coherence data for the 0.4 kg and 1.6 kg charges, totaling 8 charges with almost 200 result series, is presented. From this it can be noted that about 65 % of the compared results reach $Coh \geq 0.5$; i.e. a limit that indicates very good agreement.

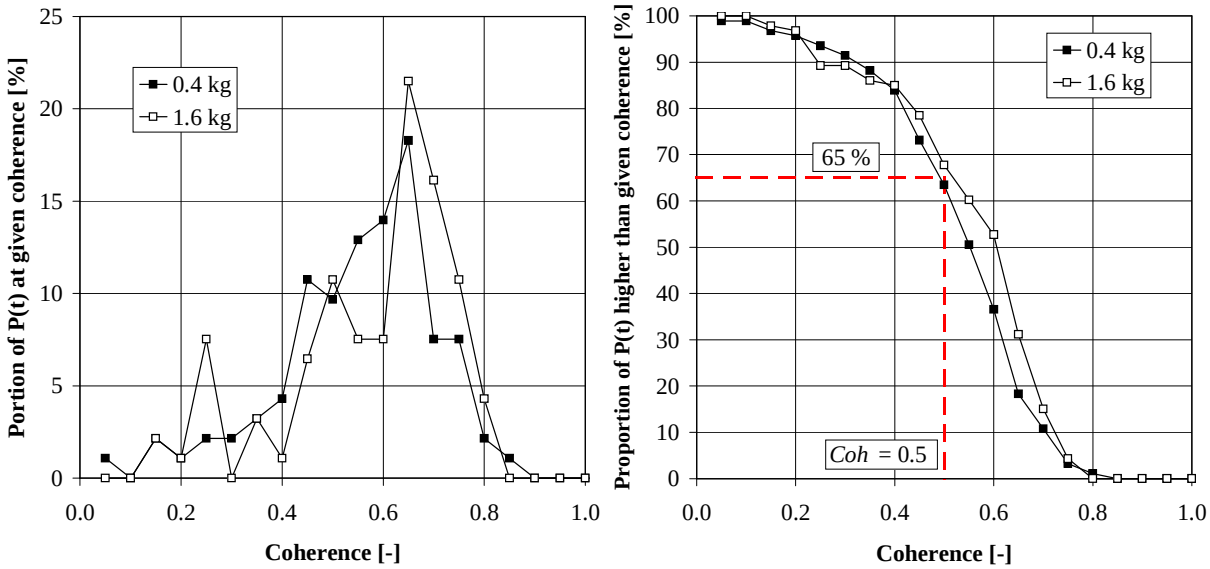

Figure 6: Coherence of 0.4 kg and 1.6 kg charges presented as portion at given coherence (left) and portion higher than given coherence (right).

SUPERPOSITIONING MODEL

Above it was shown that the prediction made in AUTODYN generally shows very good accuracy with that of the experiments. Hence, it has been confirmed that AUTODYN is a powerful tool in the prediction of load characteristics from blasts in an urban environment. The downside, though, is that programs such as AUTODYN are often expensive and demands a highly skilled user to achieve reliable results. This, in addition to the time consuming modeling and the needed CPU time to achieve the accurate results, are factors that weigh heavily against using only FE-calculations to predict blast loading on structures.

Empirical and semi-empirical methods are easier to use and also provide a basic knowledge for understanding different load situations. Such less complex methods are also needed to better understand the results from a more complex analysis, and thus prevent the latter from being transformed into a “black box”. Additionally, such simplified tools can be used to get an approximate view of the resulting load characteristics in a complex situation and could provide sufficient foundation for achieving design loads on the structures.

Based on this an attempt was made to have an engineer’s approach to the problem at hand and below a method based on [8] is presented. The concept of this method is to superpose several blast waves, where each wave is adjusted with regard to diffraction. The influence of reflected pressure is not considered, i.e. the wave characteristics are based on incident pressures only, nor is there an attempt to incorporate any confinement effects. The method is intentionally made simple since the purpose here is to provide a model that may describe the main load characteristics obtained in a complex load situation rather then a fully accurate prediction.

The resulting pressure time-relation, *P(t)*, for a general point in the geometry studied is determined performing the following four steps:

1. Derive all pressure wave paths, W_i, $1 \le i \le n$, which will be of interest for the studied point. Calculate the total distances, R_i, for each of the paths from center of charge to the studied point.
2. Use the total distances R_i in conjunction with the charge characteristics to determine the corresponding airblast parameters for both the positive and negative phase of the incident waves; i.e. arrival time t_a, incident pressures P_s^+, P_s^-, incident impulse intensities i_s^+, i_s^-, duration T^+ and T^- and the decay coefficient α.
3. Calculate the pressure time histories for incident pressures for all wave paths using

$$P_{w_i}(t) = \begin{cases} 0, \text{if } t < t_a \\ P_s^+ \left(1 - \dfrac{t - t_a}{T^+}\right) e^{-\frac{\alpha(t-t_a)}{T^+}}, \text{if } t_a \le t < t_a + T^+ \\ -P_s^- \cdot 13.9 \left(1 - \dfrac{t - (t_a + T^+)}{T^-}\right) e^{-\frac{4(t-(t_a+T^+))}{T^-}}, \text{if } t_a + T^+ \le t < t_a + T^+ + T^- \\ 0, \text{if } t \ge t_a + T^+ + T^- \end{cases} \quad (4)$$

4. The pressure-time histories for each wave W_i is multiplied with diffraction coefficients, $C_{diff,i}$, and summed together according to

$$P(t) = \sum_{i=1}^{n} C_{diff,i} \cdot P_{w_i}(t) \quad (5)$$

Blast parameters in step 2 may be determined in several ways, e.g. ConWep [4] for the positive phase. However, in order to automate the calculations as far as possible equations according to spherical burst provided in [15] were used for the positive phase. The decay coefficient α was determined in accordance with Eqs. (1) and (4), i.e. so that

$$i_s^+ = P_s^+ T^+ \left[\frac{1}{\alpha} - \frac{1}{\alpha^2}\left(1 - e^{-\alpha}\right)\right] \quad (6)$$

was fulfilled. For the negative phase, relations from [16] were used to determine the blast parameters. The influence of reflected pressure was not considered, i.e. the wave characteristics were based on incident pressures only.

The diffraction coefficients, C_{diff}, used were determined using the experimental results and comparing these to that predicted by ConWep. In [8] the diffraction coefficients were based on the peak pressure P_S^+. However, in the comparisons made herein it was found that this approach seemed to be a bit uncertain since it proved to differ somewhat also for similar load situations. Therefore, the impulse intensity i_s^+ of the first shock wave was also incorporated in the comparison, see Table 4. Due to reflections, though, it was not possible to identify the full effect of the first blast wave in the pressure-time relations obtained in the experiments, and these results were therefore not included in the comparison.

Table 4 summarizes the pressures and impulse intensities used to determine C_{diff}. Three different load situations were identified: Case 1 with diffraction around one corner to a gauge close to the edge, Case 2 with diffraction around one corner to a gauge positioned far from the edge, and Case 3 with diffraction around two corners to a gauge positioned far from the edge. Average values were determined for the diffractions coefficient when based on the pressure,

$C_{diff,P}$, and the impulse intensity, $C_{diff,I}$, and an average value of these two, $C_{diff,PI}$, was decided. It is observed that $C_{diff,P}$ and $C_{diff,I}$ deviates for Case 1 and 3 but are approximately the same for Case 2. The average diffraction coefficient $C_{diff.PI}$ is higher close to the edge (Case 1) than in the middle of the wall (Case 2), which also is in line with that observed in [8]. However, the coefficient determined based on the impulse intensity is the same, and therefore as a rough approximation it seems reasonable to use the same value $C_{diff,PI}$ for both of them. Hence, an approximate average value of C_{diff} = 0.6 is used for both Case 1 and Case 2.

It seems plausible that the resulting diffraction coefficient should depend on the number of corners that the blast wave diffracts around. Observing that the main difference between Case 2 and Case 3 is that the former diffracts around one corner while the second diffracts around two it is found that $C_{diff,3} = C_{diff,2}^{\ 2}$ seems like a good approximation. Hence, the diffraction coefficient $C_{diff,i}$ in Eq. (4) is set to $C_{diff,i} = C_{diff}^{\ m}$, where m is the number of corners that wave W_i diffracts around.

Table 4: Determination of diffraction coefficient $C_{diff,PI}$, based on experimental results and predictions made in ConWep, [4].

				Experiments		ConWep		Diffraction	
Case	Description	Gauge	R [m]	P_s^+ [kPa]	i_s^+ [Pas]	P_s^+ [kPa]	i_s^+ [Pas]	$C_{diff,P}$ [-]	$C_{diff,i}$ [-]
1	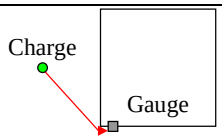	#1-BA6L	1.826	114	43.4	180	82.8	0.63	0.52
		#3-BA7L	1.826	146	43.7	180	82.8	0.81	0.53
		#4-BA7L	3.837	34.4	28.7	41.2	43.2	0.84	0.67
		Average value:		$C_{diff,P}$	**0.76**	$C_{diff,I}$	**0.57**	$C_{diff,PI}$	**0.67**
2	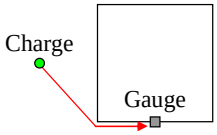	#1-BA1L	2.776	-	-	74.8	57.3	-	-
		#1-BA3L	2.776	63.2	35.5	74.8	57.3	0.84	0.62
		#1-BB1L	7.376	11.5	14.2	15.1	23.4	0.76	0.61
		#1-BB3L	7.376	11.0	11.2	15.1	23.4	0.73	0.48
		#2-BA1L	4.787	11.2	19.1	28.5	35.3	0.39	0.54
		#2-BA2L	4.787	11.9	22.9	28.5	35.3	0.42	0.65
		#2-BB1L	9.387	3.5	-	9.6	18.5	0.36	-
		#2-BB2L	9.282	4.1	10.4	11.1	18.7	0.37	0.56
		#3-BA2L	2.776	40.5	35.0	74.8	57.3	0.54	0.61
		#3-BA4L	2.776	58.0	35.7	74.8	57.3	0.78	0.62
		#3-BB2L	7.126	5.3	-	15.8	24.2	0.34	-
		#4-BA1L	4.787	11.8	19.6	28.5	35.3	0.41	0.55
		#4-BA4L	4.787	11.4	19.5	28.5	35.3	0.40	0.55
		#4-BB1L	4.787	11.6	19.3	28.5	35.3	0.41	0.55
		#4-BB2L	4.787	11.5	19.8	28.5	35.3	0.40	0.56
		Average value:		$C_{diff,P}$	**0.51**	$C_{diff,I}$	**0.57**	$C_{diff,PI}$	**0.54**
3	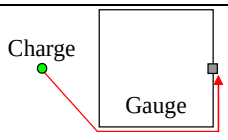	#1-BA2L	5.076	7.8	15.9	26.0	33.4	0.30	0.48
		#1-BB2L	9.676	2.3	-	10.5	18.0	0.22	-
		#3-BA1L	5.076	7.6	16.9	26.0	33.4	0.29	0.51
		Average value:		$C_{diff,P}$	**0.27**	$C_{diff,I}$	**0.49**	$C_{diff,PI}$	**0.38**

The number of blast waves used in the calculations presented herein is limited to six. Further, when determining the distances R_i an approximate approach was used based on simple geometrical assumptions regarding angles of reflection; the difference in distance obtained being rather negligible. An example of how the different shock waves are determined and put together in a resulting pressure-time relation is shown in Figure 7 and Table 5. When determining the blast parameters a spherical air burst was assumed. However, since the current load case is more similar to that of a hemispherical airburst the charge weight was increased with a factor 1.8 due to mirroring, [17].

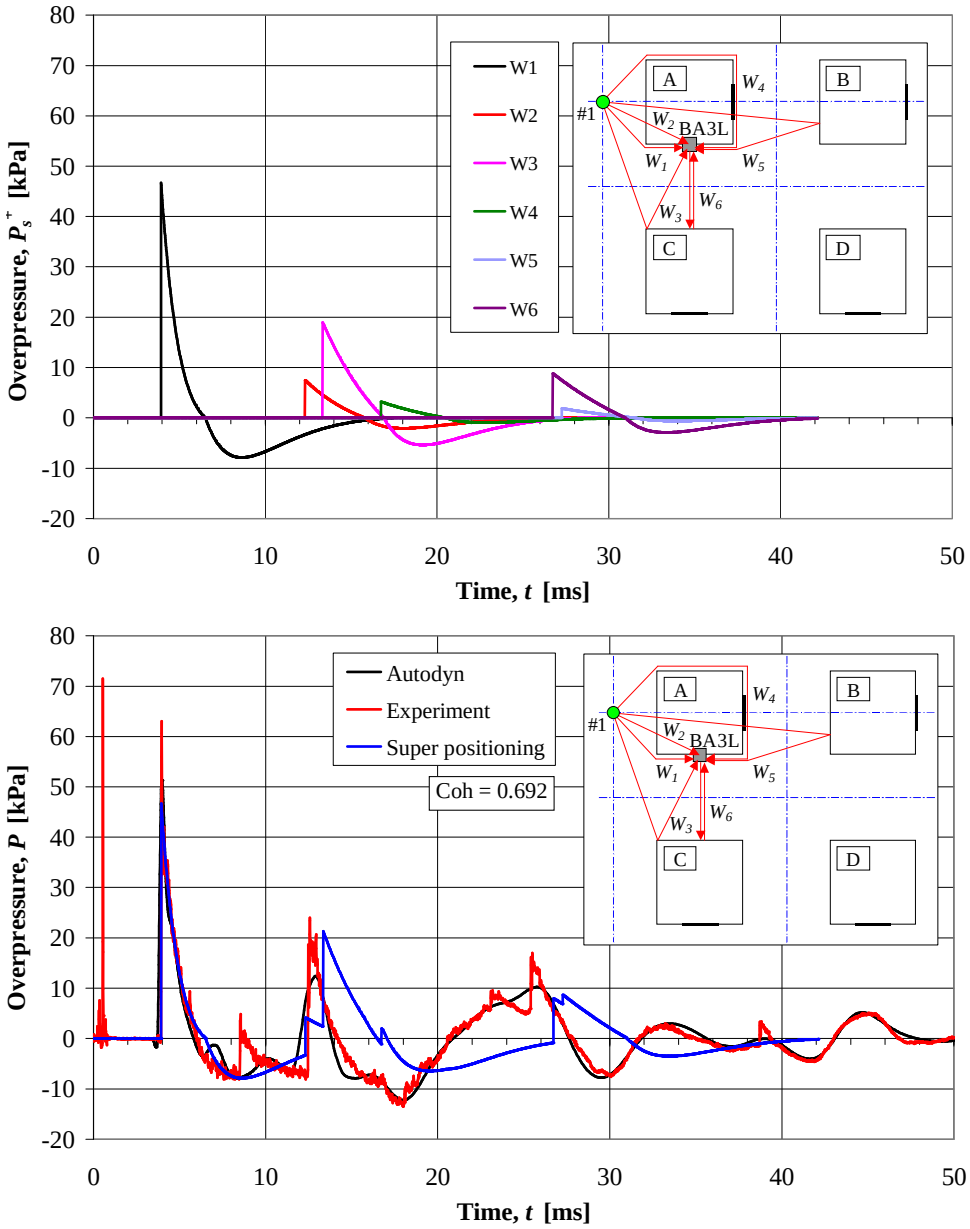

Figure 7: (Top) The six shock wave paths W_1 - W_6, multiplied with C_{diff}, that affect the studied point BA3L, and (bottom) comparison with the results from AUTODN and the experiments. The correlation between AUTODYN and experiments resulted in Coh = 0.692.

Table 5: Input data according to Eqs. (4) and (5) for the shock waves shown in Figure 7 The data is based on a spherical airburst using a scaled distance Z based on an equivalent weight of 1.21 and a mirror coefficient of 1.8.

	Geometry		Positive phase					Negative phase			Diffraction	
Wave	R	Z	t_a	P_s^+	i_s^+	T^+	α	P_s^-	i_s^-	T^-	m	C_{diff}
	[m]	[m/kg$^{1/3}$]	[ms]	[kPa]	[Pas]	[ms]	[-]	[kPa]	[Pas]	[ms]	[#]	[-]
W_1	2.78	3.06	3.932	78.5	60.4	2.591	1.81	-13.1	-66.0	10.980	1	0.60
W_2	5.85	6.44	12.311	20.8	30.6	3.481	0.52	-5.8	-31.0	11.769	2	0.36
W_3	6.21	6.84	13.350	19.0	29.0	3.552	0.47	-5.4	-29.2	11.834	0	1.00
W_4	7.38	8.12	16.738	14.8	24.6	3.759	0.37	-4.5	-24.5	12.026	3	0.22
W_5	10.99	12.10	27.268	8.6	16.8	4.246	0.26	-2.9	-16.4	12.481	3	0.22
W_6	10.81	11.90	26.735	8.8	17.1	4.225	0.28	-2.9	-16.6	12.461	0	1.00

In Figure 8 some further comparisons between experiments, AUTODYN and the super positioning method are illustrated. The correlations of the shown results, based on the positive and negative impulse intensities, are summarized in Table 6.

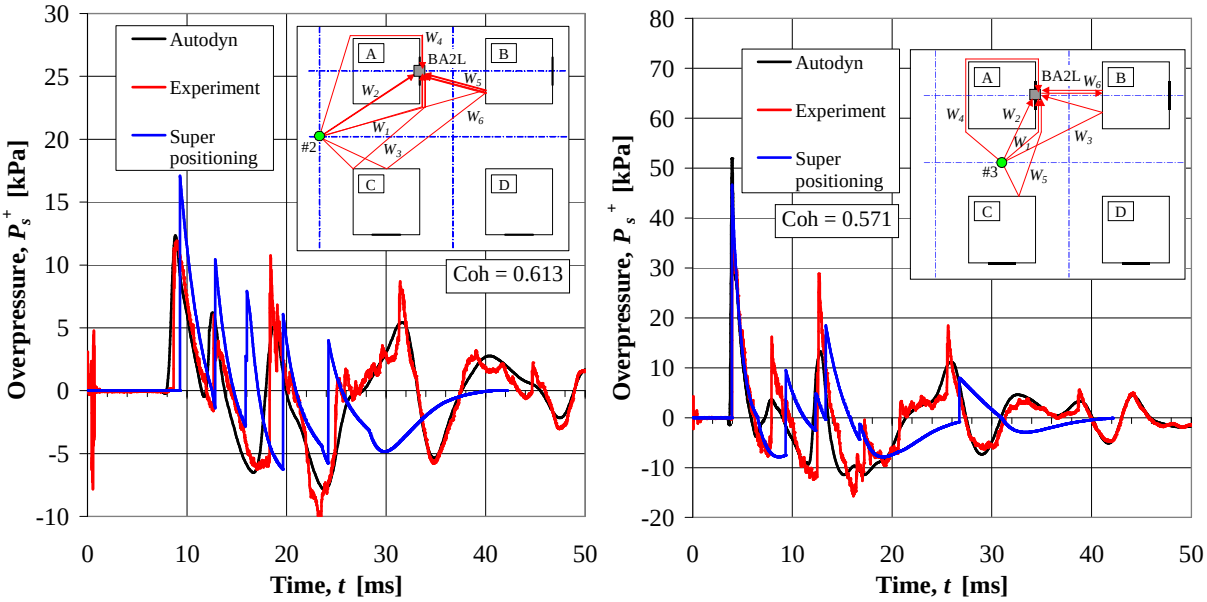

Figure 8: Comparison of pressure-time relation from AUTODYN, experiments and super positioning method: #2-BA2L (left) with *Coh* = 0.613, and #3-BA2L, with *Coh* = 0.571.

Table 6: Comparison of total positive and negative impulse intensities in experiments, AUTODYN and super positioning method according to Eqs. (1) and (2) when t_{end} = 40 ms.

	#1-BA3L				#2-BA2L				#3-BA2L			
Source	i_s^+	i_s^-	γ^{+} 1)	γ^{-} 2)	i_s^+	i_s^-	γ^{+} 1)	γ^{-} 2)	i_s^+	i_s^-	γ^{+} 1)	γ^{-} 2)
	[Pas]	[Pas]	[-]	[-]	[Pas]	[Pas]	[-]	[-]	[Pas]	[Pas]	[-]	[-]
Experiment	98.2	-101.2	1.00	1.00	52.8	-56.4	1.00	1.00	102.7	-100.2	1.00	1.00
Autodyn	99.8	-105.3	1.02	1.04	52.6	-58.8	1.00	1.04	105.1	-100.0	1.02	1.00
Super positioning	89.2	-92.5	0.91	0.91	41.0	-53.3	0.78	0.95	80.7	-84.6	0.79	0.84

1) $\gamma^+ = i_s^+ / i_{s\,Exp}^+$ 2) $\gamma^- = i_s^- / i_{s\,Exp}^-$

Even though the general pressure-time behavior does not fully correspond with the experimental one for the whole time domain it still generates a good view of the load characteristics obtained. The ratios γ^+ and γ^- presented in Table 6 shows that the total impulse intensities predicted by this simplified model is rather correct, the discrepancy being only about 10-20 %. Hence, the good correlation in the comparisons made above suggest that the super positioning method presented herein represent a simplified approach that yields results fairly close to that observed in reality.

CONCLUSIONS

An experimental and numerical study of blast load at an intersection was carried out. The load effects of two types of charges, 0.4 kg and 1.6 kg PETN, positioned in four different locations were simulated using the explicit code AUTODYN and compared to the experimental results. All AUTODYN analyses were made before the experiments were carried out, and hence the results presented herein are used to validate AUTODYN's ability to describe the blast behavior in an urban environment. An automatic remapping routine was developed for the blast simulations in AUTODYN. This routine enabled automatic detection of the shock front close to a boundary, and thus a criterion for when in time to initiate the remapping process, allowing a more time efficient approach to large blast simulations in a complex environment.

It is shown that the agreement between the results obtained in the experiments and the AUTODYN simulations generally is very good. A coherence measure is introduced for comparing experimental and numerical results and it is concluded that this is a convenient method to get an estimation of how well the results coincide. For the results presented herein it is shown that about 65 % of the compared measurements fulfill $Coh \geq 0.5$, i.e. a the limit that indicates very good agreement. For gauges where the pressure was low, less than about 50-100 kPa, the agreement generally went from very good to excellent. Consequently, it is concluded that AUTODYN manage very well to describe the resulting blast effects and that it with confidence may be used as a powerful tool when studying blast loads in a complex urban environment.

An approach for a simplified technique, using super position of several incident shock waves, to estimate the blast load in a more complex environment is presented and compared to the experimental and numerical results. It is found that the method, despite its simplicity and rather crude approach, manage rather well to describe the general behavior of the resulting load characteristics observed in experiments and numerical analyses. The results presented herein show a deviation of just about 20 % compared to that in the experiments.

ACKNOWLEDGEMENTS

The authors thankfully acknowledge the Swedish Rescue Services Agency (Räddningsverket) for the financing of the research project *Resistance capacities of buildings for extreme dynamic loading*. Special thanks are due to Björn Ekengren for his invaluable support; without him this project had not been the same. Further thanks are due to the Norwegian Defence Estates Agency (Forsvarsbygg), especially Svein Christensen and Ståle Skudal, for their initiation, invitation to take part in and financial support of the experimental work presented herein. Additionally, the Swedish Defence Research Agency (FOI), of whom Richard Forsén, Anders Carlberg and Roger Berglund are thanked, for their part in the experimental performance. Finally, thanks to Bert von Rosen, Canadian Explosives Research Laboratory, for providing help with the super positioning method presented herein.

REFERENCES

[1] Ekengren, B., 2006, Skyddsrum, SR 06 (Civil defence shelters, SR 06, in Swedish), Swedish Rescue Services Agency, B54-141/06, Karlstad, Sweden.

[2] Johansson, M. and Laine, L., 2006, Resistance capacities of buildings for extreme dynamic loading, Research project description, Swedish Rescue Services Agency, http://www.srv.se/templates/SRV_Page____15919.aspx, Karlstad, Sweden.

[3] Remennikov, A.M., 2003, A review of methods for predicting bomb blast effects on buildings, Journal of Battlefield Technology, 6(3), pp. 5–10.

[4] ConWep, 1992, ConWep – Collection of conventional weapons effects calculations based on TM 5-855-1, Fundamentals of Protective Design for Conventional Weapons, U.S. Army Engineer Waterways Experiment Station, Vicksburg, USA.

[5] Rose, T.A. and Smith, P.D., 2002, Influence of the principal geometrical parameters of straight city streets on positive and negative phase blast wave impulses, International Journal of Impact Engineering, 27, pp. 359–376.

[6] Rose, T.A. and Smith, P.D., 2003, The influence of street junctions on blast wave impulses produced by vehicle bombs, Proceedings of the 11th International Symposium on Interaction of the Effects of Munitions with Structures, Mannheim, Germany.

[7] Dörr, A., Brombacher, B., Gürke, G., 2004, Blast behind street junctions originating from vehicle bombs, Proceedings of 18th Symposium on the Military Aspects of Blast and Shock, Bad Reichenhall, Germany.

[8] von Rosen, B., Guilbeault, E., Contesabile, E., 2004, A preliminary investigation into the interaction of shock waves behind a simple rectangular structure, Proceedings of 18th Symposium on the Military Aspects of Blast and Shock, Bad Reichenhall, Germany

[9] Remennikov, A.M. and Rose, T.A., 2005, Modelling blast loads on buildings in complex city geometries," Computers and Structures, 83, pp. 2197-2205.

[10] Smith, P.D. and Rose, T.A., 2006, Blast wave propagation in city streets – an overview, Prog. Struct. Engng Mater. 8, pp. 16-28.

[11] Century Dynamics Inc., 2004, AUTODYN Theory Manual Revision 5.0, San Ramon, CA, USA.

[12] Johansson, M. and Laine, L., 2007, Bebyggelsens motståndsförmåga mot extrem dynamisk belastning, Delrapport 1: Last av luftstötvåg (Resistance capacities of buildings for extreme dynamic loading, Report 1: Load from airblast, in Swedish.), Swedish Rescue Services Agency, B54-232/07, Karlstad, Sweden.

[13] Johansson, M. and Laine, L., 2008, Bebyggelsens motståndsförmåga mot extrem dynamisk belastning, Delrapport 2: Explosion i gatukorsning (Resistance capacities of buildings for extreme dynamic loading, Report 2: Explosion at an intersection, in Swedish.), Swedish Rescue Services Agency, to be published in 2008, Karlstad, Sweden.

[14] Johansson, M., Larsen O.P., Laine, L., 2007, Explosion at an intersection in an Urban Environment – Experiments and analyses, Proceedings of the 78th Shock and Vibration Symposium, Philadelphia, PA, USA.

[15] Kingery, C.N., Bulmash, G., 1984, Airblast Parameters from TNT Spherical Air Burst and Hemispherical Surface Burst, Ballistic Research Laboratory, Aberdeen Proving Ground, Technical Report ARBRL-TR-02555, Maryland, USA.

[16] Departments of Special Weapons Agency (DSWA), Army, Navy, and Air Force, 1998, Protective Structures Automated Design System (PSADs), Version 1.0, U.S. Army Corps of Engineers: ATTN: CEMP-ET 20, USA.

[17] Baker, W.E., Cox, P.A. Westine, P.S., Kulesz J.J. Strehlow R.A., 1983, Explosion Hazards and Evaluation, Elsevier Scientific Publishing Company, New York, NY, USA.